DOI 10.1007/s10517-020-04750-8

Distribution and Migration of Human Placental Mesenchymal Stromal Cells in the Brain of Healthy Rats after Stereotaxic or Intra-Arterial Transplantation

K. K. Sukhinich[1], D. D. Namestnikova[3], I. L. Gubskii[6], A. N. Gabashvili[4], P. A. Mel'nikov[5], E. Ya. Vitushev[4], D. A. Vishnevskii[3], V. A. Revkova[7], A. A. Solov'eva[3,6], K. S. Voitkovskaya[3], I. V. Vakhrushev[2], V. V. Burunova[2], A. B. Berdalin[6], M. A. Aleksandrova[1], V. P. Chekhonin[3,5], L. V. Gubskii[3,6], and K. N. Yarygin[2,8]

Translated from *Kletochnye Tekhnologii v Biologii i Meditsine*, No. 4, pp. 227-237, December, 2019
Original article submitted September 3, 2019

Human placenta mesenchymal stromal cells were injected to healthy rats either stereotaxically into the striatum or intra-arterially through the internal carotid artery. Some cells injected into the brain migrated along the corpus callosum both medially and laterally or concentrated around small blood vessels. A small fraction of MSC injected intra-arterially adhered to the endothelium and stayed inside blood vessels for up to 48 hours mostly in the basin of the middle cerebral artery. Neither stereotaxic, nor intra-arterial transplantation of mesenchymal stromal cells modulated the proliferation of neural stem cells in the subventricular zone of the brain, but stereotaxic transplantation suppressed activation of their proliferation in response to traumatization with the needle.

Key Words: *mesenchymal stem cells; cell migration; intra-arterial transplantation; intracerebral transplantation; subventricular zone*

Mesenchymal stromal cells (MSC) are widely used in the development of methods of cell therapy for CNS pathologies [13,17,29]. Preclinical studies of the safety, efficacy, and mechanisms of action of biomedical products based on MSC include testing on intact animals and animals with model pathologies that simulate human diseases. In particular, analysis of migration and homing of transplanted cells in the brain and other organs is important for understanding of the mechanisms of their therapeutic and possible side effects. However, not so many studies focused on the distribution and effects of cells transplanted to intact animals. Usually, the data obtained on intact animals are included as the control in reports on the effects of cell therapy in modeled pathologies. In many cases, this is because these data appear as being of little interest. In our opinion, the interaction of transplanted MSC with recipient's body is of great interest not only for the development of biomedical products, but also for basic science. The basic mechanisms of body response to cell transplantation can be studied on intact animal.

Here we performed a comparative analysis of the distribution and migration of MSC isolated from the human placenta after stereotaxic or intra-arterial administration to healthy rats and evaluated the effect

[1]N. K. Koltsov Institute of Developmental Biology, Russian Academy of Sciences; [2]V. N. Orekhovich Research Institute of Biomedical Chemistry; [3]N. I. Pirogov Russian National Research Medical University; [4]N. I. Vavilov Institute of General Genetics, Russian Academy of Sciences; [5]V. P. Serbsky National Medical Research Center of Psychiatry and Narcology, Ministry of Health of the Russian Federation; [6]Federal Center of Cerebrovascular Pathology and Stroke, Ministry of Health of the Russian Federation; [7]Federal Research and Clinical Center, Federal Medical-Biological Agency; [8]Russian Medical Academy of Continuous Professional Education, Ministry of Health of the Russian Federation, Moscow, Russia. ***Address for correspondence:*** sukhinichkirill@gmail.com. K. K. Sukhinich

of MSC transplantation on proliferative activity of cells (presumably neural stem cells) in the neurogenic subventricular zone (SVZ) of the lateral ventricles.

MATERIALS AND METHODS

Isolation of cell culture. MSC were isolated from normal human placenta (38-40 weeks gestation) according to the standard protocol [21]. Informed consent for sampling and use of biological material for scientific purposes was signed by all women. Placental fragments were washed with Hanks saline (PanEco), pipetted, and incubated with 0.1% collagenase I (Gibco) for 30 min at 37°C. The resultant suspension was centrifuged (300*g*, 10 min), the supernatant was discarded, and the precipitate was resuspended in growth medium. The cells were cultured in DMEM/F-12 medium supplemented with 2 mM glutamine, 100 U/ml penicillin, 0.1 mg/ml streptomycin (Gibco), and 10% fetal calf serum (HyClone) under standard conditions (37°C, 5% CO_2) in 75 cm^2 vials for 3 days. Non-adherent cells were removed during medium changing. After attaining 80% confluence, the cells were harvested with 0.25% trypsin-EDTA (Gibco) and subcultured 1:4.

Cell labeling. Fluorescent labeling was performed using superparamagnetic iron oxide microparticles (SPIO, MC03F Bangs Laboratories, mean diameter 0.50-0.99 μ) carrying fluorescent dye Dragon Green (λ_{ex}=480 nm, λ_{em}=520 nm) and membrane lipophilic dye PKH26 (Sigma-Aldrich; λ_{ex}=551 nm, λ_{em}=567 nm). Two variants of labeled cells were used for experiments: cells labeled with only Dragon Green-loaded iron particles and cells additionally labeled with PKH26.

MSC were labeled with iron oxide particles when the cultures attained 80-90% confluence. The cells were incubated with particles (5 μl particle suspension per 1 ml growth medium) for 12 h under standard conditions, then washed twice with Hanks saline to remove particles that were not captured by the cells. Then, MSC were removed from plastic by trypsinization.

For labeling with PKH26 dye, cells were removed from plastic, washed with serum-free growth medium, centrifuged (500*g*, 5 min), and the supernatant was removed. MSC were resuspended in 1 ml Diluent C solution, mixed with 1 ml Diluent C solution containing 4 μl PKH26, and incubated for 5 min. Reaction was stopped by adding an equal volume of fetal calf serum.

Laboratory animals. The experiment was performed on male Wistar rats (*n*=51) weighing 230-300 g. All manipulations with laboratory animals were approved by the Ethical Committee of N. I. Pirogov Russian National Research Medical University and performed in compliance with the European Council Directive 2010/63/EEC. The animals were randomly divided into the following groups: group 1 rats received stereotaxic injection of MSC (*n*=26; in 5 rats, cell proliferation in SVZ was evaluated); group 2 rats received intra-arterial injection of MSC (*n*=11; 5 animals were used for evaluation of cell proliferation in SVZ); group 3 rats received stereotaxic injection of physiological saline (PS; *n*=5; cell proliferation in SVZ was assessed in all animals); group 4 rats received intra-arterial injection of PS (*n*=3; cell proliferation in SVZ was assessed in all animals); group 5 comprised intact rats (*n*=5; cell proliferation in SVZ was assessed in all animals). The animals were sacrificed by intraperitoneal injection of a lethal dose of chloral hydrate.

Intracerebral and intra-arterial transplantation. The surgery was performed under inhalation isoflurane anesthesia (1.5-2%+98% air) with intraperitoneal premedication with atropine sulfate (0.05 mg/kg in 1 ml saline) and local subcutaneous anesthesia with 0.1 ml of 0.5% bupivacaine solution. The transplantation technique was described in detail earlier [21]. For intracerebral injection of MSC, the rats were fixed in a stereotaxis with the AngleTwo computer navigation system (Leica), the skin was cut, the skull was scalped, and a trepanation hole (diameter 1 mm) was drilled at the following coordinates from the bregma: +0.6 mm AP (anteroposterior direction), +3.5 mm ML (medial-lateral), and -4.5 mm VD (ventral-dorsal). The transplant (3×10^5 MSC or saline) in a volume of 15 μl was injected into the striatum of the right hemisphere at a rate of 3 μl/min with a Hamilton 500 μl syringe fixed in a microinjector (KD Scientific). In 5 min, the needle was slowly removed and the wound was sutured.

For intra-arterial administration. the skin of the neck was cut along the midline, the right common (CCA), external (ECA), and internal (ICA) carotid arteries were isolated and the pterygopalatine artery was ligated. A polyurethane microcatheter (Braintree Scientific, MTV 1, outer diameter 0.33 mm) filled with PS was introduced to 5-8 mm through the incision on the ECA into the CCA. The transplant (5×10^5 MSC or PS) in a volume of 1 ml was injected with a microinjector at a rate of 100 μl/min. Slow continuous infusion and preserved blood flow around the catheter are important conditions for safe intra-arterial transplantation without embolic complications [22]. After the end of infusion, the catheter was removed, the ligature around the ECA stump was tightened, and the wound was sutured with intermittent nodular suture. After all manipulations, 0.2 ml gentamicin solution was injected intramuscularly, and the animals were placed in a heated cage (37°C) to recover from anesthesia.

MRI. Dynamic MR study was performed on a 7T ClinScan MRI scanner for small laboratory animals (Bruker BioSpin) using a phase array four elements rat brain coil. During scanning, the animals were under inhalation anesthesia as described above. Anatomical T2-weighted images based on Turbo Spin Echo pulse sequence with restore magnetization pulse and spectral fat saturation were acquired (turbo factor=9; TR/TE=4000/46 msec; number of averages=2; field of view 37×29.6 mm; slice thickness 0.5 mm; matrix size 320×256). For visualization of MSC labeled with iron oxide microparticles, susceptibility weighted imaging (SWI) based on 3D gradient echo sequence with flow compensation, RF spoiling, and spectral fat saturation was used (TR/TE=50/19.1 msec; angle=15; number of averages=1; field of view 30×20.6 mm; slice thickness 0.5 mm; matrix size 256×176). In experiments with intra-arterial injections, diffusion-weighted images with calculation of apparent diffusion coefficient maps were acquired to identify possible embolic complications and foci of acute cytotoxic edema in the brain substance (based on echo-planar pulse sequence with spectral fat saturation, TR/TE=9000/33 msec; b-factors=0 and 1000 sec/mm^2; number of diffusion directions=6; number of averages=3; field of view 30×19.5 mm; slice thickness 1.0 mm; matrix size 86×56).

Histology. The distribution and migration of MSC were analyzed by histological methods on days 1, 2, 3, 7, and 15 and proliferation of endogenous cells in SVZ was assessed on day 15. Animals were euthanized with a lethal dose of chloral hydrate and transcardial perfusion with 4% paraformaldehyde on 0.01 M PBS (pH 7.4) was performed. The brain was extracted and placed in 4% paraformaldehyde for 24 h, then frontal 50-μ sections of the brain were sliced using a vibratome (Thermo Scientific, micron HM 650v). SPIO-labeled cells were identified by staining after Perls (qualitative reaction to iron). To this end, the preparations were incubated with 2% potassium ferrocyanide and 2% hydrochloric acid for 10 min, then washed in distilled water; the nuclei were poststained with neutral red. For immunohistochemical staining, the brain sections were incubated for 24 h in 0.01 M PBS (pH 7.4) with 0.3% Triton X-100 and 5% normal goat serum (Sigma-Aldrich) and then for 24 h in 0.01 M PBS (pH 7.4) with 0.3% Triton X-100, 5% normal goat serum (Sigma-Aldrich), and primary antibodies: anti-alpha SMA antibody (1:500; Abcam), anti-Rat Blood-Brain Barrier Antibody (1:100; BioLegend), anti-Ki67 (1:200; Abcam). The sections were washed in 0.01 M PBS (pH 7.4) and incubated in 0.01 M PBS (pH 7.4) with 0.3% Triton X-100 and secondary goat antibodies to rabbit immunoglobulins (1:500; Alexa Fluor 647 or Alexa Fluor 594; Sigma-Aldrich) or mouse immunoglobulins (1:500; Alexa Fluor 647; Sigma-Aldrich). Then washed in 0.01 M PBS (pH 7.4), the nuclei were poststained with DAPI (2 μg/ml; Sigma); the sections were mounted under coverglass in glycerin. In sections not incubated with antibodies, the nuclei were also stained with DAPI (2 μg/ml; Sigma).

Microscopy and image processing. The preparations were photographed under a Keyence BZ-9000E digital fluorescence microscope and a Nikon A1R MP+ laser scanning confocal microscope. Migration of transplanted cells was assessed as the distance (in μ) between the site of transplantation and cells located at the maximum distance from this site. Proliferative activity of recipient cells in SVZ was assessed by the count of Ki-67$^+$ cells in the right hemisphere. To this end, 4-6 sections were selected in the interval from +0.8 to -0.8 from bregma (from the anterior, median, and posterior of parts of SVZ, respectively); three regions were scanned in each section under a confocal microscope. The obtained Z-stacks were analyzed using Fiji Cellcounter plugin. This approach allowed calculating the number of cells in the entire volume of each 50-μ section.

Statistical analysis. The results were processed using SPSS Statistics 23.0 (IBM) and R software 3.5.3. (R Foundation for Statistical Computing) software. Quantitative data (distance of migration of labeled MSC; number of Ki-67$^+$ cells) were presented as mean and standard deviation and as the median and the lower and upper quartiles. Null hypothesis was rejected at $p<0.05$. Migration distance in the groups was compared using the Mann—Whitney test. For evaluation of proliferation of endogenous cells in SVZ, two-way ANOVA with linear mixed model was used with adjustment for transplanted substance (MSC/PS) and type of transplantation (stereotaxic/intra-material).

RESULTS

We performed a comparative analysis of the distribution and migration of MSC isolated from the human placenta after their stereotaxic and intra-arterial transplantation into the brain of healthy rats and evaluated the influence of MSC transplantation on proliferation activity of cells (presumably neural stem cells) in SVZ of the lateral ventricles, which is a neurogenic zone [23]. It should be noted that immunosuppression was not performed, because MSC are characterized by low immunogenicity and ability to limit the immune response and inflammation [24], and hence can be used not only for allogeneic, but also for xenogeneic transplantation.

Distribution of MSC after intracerebral transplantation. MSC labeled with magnetic iron oxide microparticles (SPIO) conjugated with a green fluo-

rescent protein were introduced stereotaxically into the right striatum. For evaluation of cell migration, *in vivo* MRI scanning was performed in the dynamics starting from day 1 to day 15 after transplantation; he data were confirmed by histological examination (Fig. 1). As was previously shown [21], SPIO-labeled MSC can be visualized by MRI using various pulse sequences; the most sensitive is SWI mode, which allows visualization of small groups of cells or even single cells. In MR images of rat brain, labeled MSC looked as hypointensive zones at the site of transplantation (Fig. 1, *b*, *e*, *i*). It should be noted that the size of the hypointensive zone in SWI images significantly exceeds the actual volume occupied by stereotaxically injected cells (15 µl), because SWI sequence is highly sensitive to distortion of the local magnetic field caused by accumulation of labeled MSC in a small volume. Additionally, less sensitive T2-weighted images were analyzed to clarify the distribution and migration of cells in the studied anatomical regions (Fig. 1, *c*, *g*, *k*). MRI data were verified by histological examination. Confocal microscopy was used to visualize fluorescent label (Fig. 1, *a*, *d*, *h*), and bright-field microscopy to detect iron particles stained after Perls (Fig. 1, *f*, *j*).

At all stages, the transplant was accurately detected by MRI and histological examination; it was located along the needle track in the cortex, corpus callosum, and striatum. In the cortex and striatum, most transplanted cells were located compactly along the needle track, and only solitary cells migrated to the brain parenchyma (Fig. 1). A similar location of the transplant was described is a previous study [6], where virtually no migration of transplanted MSC in the basal nuclei was observed in healthy brain. However, in our experiment, distant migration was observed in the area of the corpus callosum both medially (*i.e.* towards the left ventricle; Fig. 1, *d*-*g*) and laterally from the injection

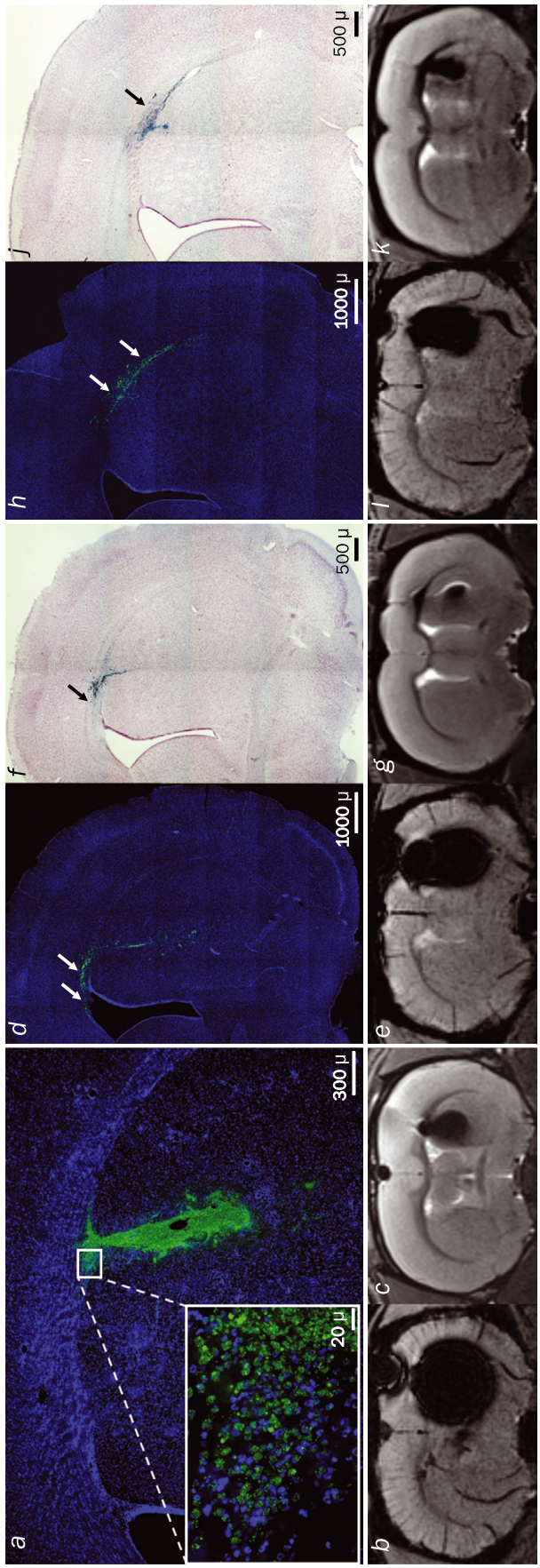

Fig. 1. Migration of MSC after intracerebral administration to healthy rats. Results of MRI and histological examination of brain sections on days 1 (*a*-*c*) and 15 (*d*-*k*) after transplantation. Epifluorescence microscopy (*a*), MR image in SWI mode (*b*, *e*, *i*), T2-weighted image (*c*, *g*, *k*), confocal microscopy (*d*, *h*), bright-field microscopy: Perls staining (*f*, *j*). *a*) Green fluorescence corresponds to SPIO-labeled cells. MSC are located compactly in the striatum, single cells migrate from the transplant to the brain parenchyma. Migration through the corpus callosum in the medial and lateral directions. *b*, *c*) Hypointensive area corresponds to the MSC transplantation zone. *d*, *e*) Migration of SPIO-labeled cells along the corpus callosum towards the lateral ventricle. MSC are visualized in contact with SVZ. *f*) Blue color corresponds to the locations of SPIO clusters. *g*) The decrease in signal intensity in the area of the corpus callosum corresponds to MSC migration zone. *h*, *i*, *j*) Migration of SPIO-labeled cells along the corpus callosum laterally from the insertion track. *k*) Reduced signal intensity in the area of the corpus callosum corresponds to MSC migration zone laterally from the injection track.

track (Fig. 1, *h-k*). The mean distance of maximum migration in the lateral and medial directions was 333±76 and 376±25 μ, respectively, on day 1, 590±295 and 586±306 μ on day 7, and 1036±421 and 1018±264 μ on day 15. No significant differences in the distance of cell migration along the corpus callosum between lateral and medial directions were revealed. Moreover, we showed that a significant portion of transplanted cells were visualized around cerebral vessels from their outer side (Fig. 2) both in the striatum and in the corpus callosum at all stages of the study. It is likely that MSC migration is guided by white matter axons and blood vessels [15]. A similar phenomenon was reported for other types of stem cells [19,28]. MSC distribution in the corpus callosum was also shown in animals with modeled brain injury and infarction; in this case, MSC migration to the lesion focus was more pronounced than in healthy rats [11,12].

MSC distribution after intracerebral transplantation. During intra-arterial transplantation, labeled cells were injected into the right ICA with a microinjector at a rate of no more than 100 μl/min and with maintenance of blood flow around the catheter. We have previously demonstrated that these conditions are safe and allow preventing embolism of small rain vessels [22]. Immediately after intra-arterial administration, all rats underwent an MRI study with diffusion-weighted images to exclude ischemic brain damage caused by vascular occlusion with transplanted cells. No complications caused by transplantation procedure were revealed. Cell distribution in the brain was evaluated using susceptibility-weighted images and verified by histological examination. Immediately after injection into the right ICA, the cells were distributed in the ipsilateral hemisphere: most cells were located in the motor and sensory cortex (Fig. 3, *b*, *c*), hippocampus (Fig. 3, *b*), and also in the striatum, thalamus, and hypothalamus. Solitary cells were also seen in the contralateral hemisphere, more often in the frontal cortex and rostral part of the striatum. It can be hypothesized that the cell distribution is largely determined by anatomy of cerebral vessels (blood flow through anastomoses and the Willis circle, diameter of vessels and their distance from the ICA trunk) and, as a consequence, intensity of perfusion in this or that part of the brain. The above-listed structures belong to the basin of the middle cerebral and common anterior cerebral arteries, and the hippocampus, thalamus, and hypothalamus are supplied simultaneously through the posterior cerebral, anterior choroidal, and thalamic arteries. According to the results of histological examination and MRI in dynamics (Fig. 3), the number of labeled MSC in the brain gradually decreased, and on day 3, no transplanted cells were detected. After intra-arterial administration, most MSC were located inside the cerebral vessels, which was confirmed by immunohistochemical analysis (Fig. 4). As transplanted MSC closely contacted with the vascular walls, we cannot exclude that single cells can cross the blood—brain barrier (BBB) and migrate into the brain parenchyma. Migration of MSC through BBB was shown in studies performed on monolayer cultures of cerebral vascular endothelium [18,27]. Two potential mechanisms of MSC penetration through BBB are described: paracellular migration involving disruption of tight junctions and transcellular migration through pores formed directly in endotheliocytes, without affecting cell—cell contacts (this mechanism is described in more detail in review [10] and in relation to white blood cells [4]). It should be taken into account that BBB is a complex structure formed by the not only endotheliocytes, but also astrocytes, pericytes, and neurons [1]. In light of this, *in vitro* models cannot fully reproduce BBB cytoarchitectonics and functioning. Homing of MSC in the lesion focus after systemic administration was demonstrated [7]; however, passive cell penetration through BBB in sites where its structure is violated cannot be excluded. Thus, MSC capacity to pass through the BBB *in vivo* requires further study. The regularities and mechanisms of cell distribution in the brain after systemic administration are not completely understood. It remains unclear whether MSC possess mechanisms underlying their active homing in the lesion focus and/or certain brain structures, or they are "trapped" in capillaries along the blood flow [16]. Interestingly, some studies [9,20] demonstrated similar distribution of MSC after intra-arterial administration in both healthy animals and animals with modeled brain infarction. Immediately after transplantation, the cells were visualized in the ipsilateral hemisphere inside the vessels, where they remained for a short time, while in 24 h, most cells disappeared from the cerebral vessels and were found in the lungs and other parenchymal organs. This disappearance of MSC from brain structures occurred somewhat faster after xenogeneic transplantation (injection of human MSC to rats) than in allogeneic transplantation [9]. However, in this study, human MSC were present inside rat cerebral vessels up to 2 days.

Proliferation of endogenous cells in SVZ. Proliferative response of endogenous cells in SVZ was evaluated in 15 days after MSC transplantation (Fig. 5). Experimental data were evaluated using two-was ANOVA. Laboratory animals received injection of MSC or PS (factor: type of administered substance) via two routes: intra-arterially or stereotaxically (factor: administration route). At the end of the experiment, proliferating cells were detected by immunohistochemical staining with antibodies to Ki-67; this antigen is present in cell nucleus in all phases

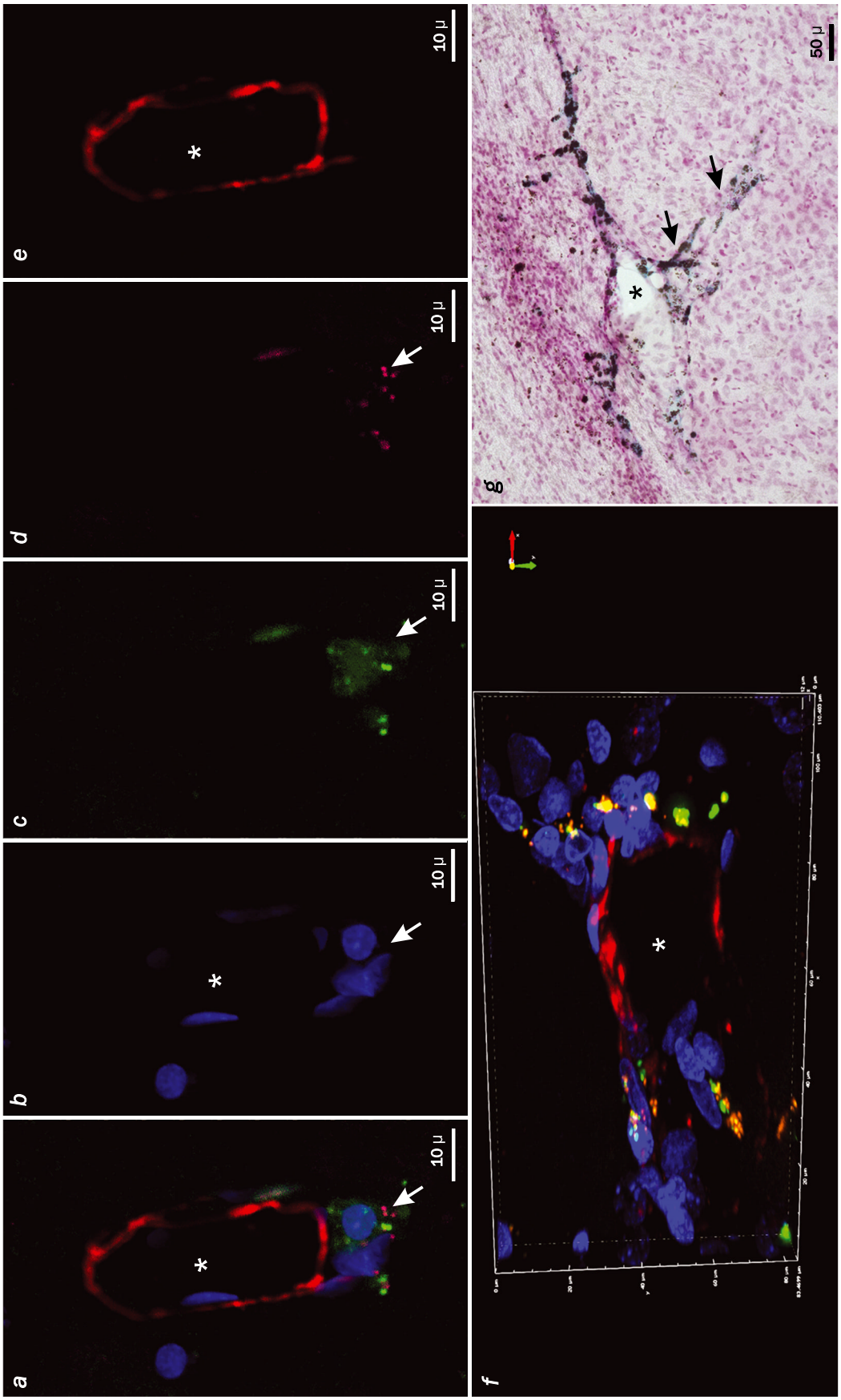

Fig. 2. Migration of MSC along blood vessels after intracerebral administration to healthy rats. On day 7 after transplantation, MSC labeled with SPIO and lipophilic membrane dye PKH26 are visualized around cerebral vessels in contact with their outer walls. *a*) Combination of images *b-d*: DAPI+SPIO+PKH26+αSMA; *b*) DAPI; *c*) SPIO; *d*) PKH26; *e*) αSMA. *f*) 3D visualization of cells around blood vessel (image parameters: width 110.4 μ, height 83.47 μ, thickness 12 μ). *g*) Perls staining. Arrows show transplanted cells, asterisks show vascular lumen.

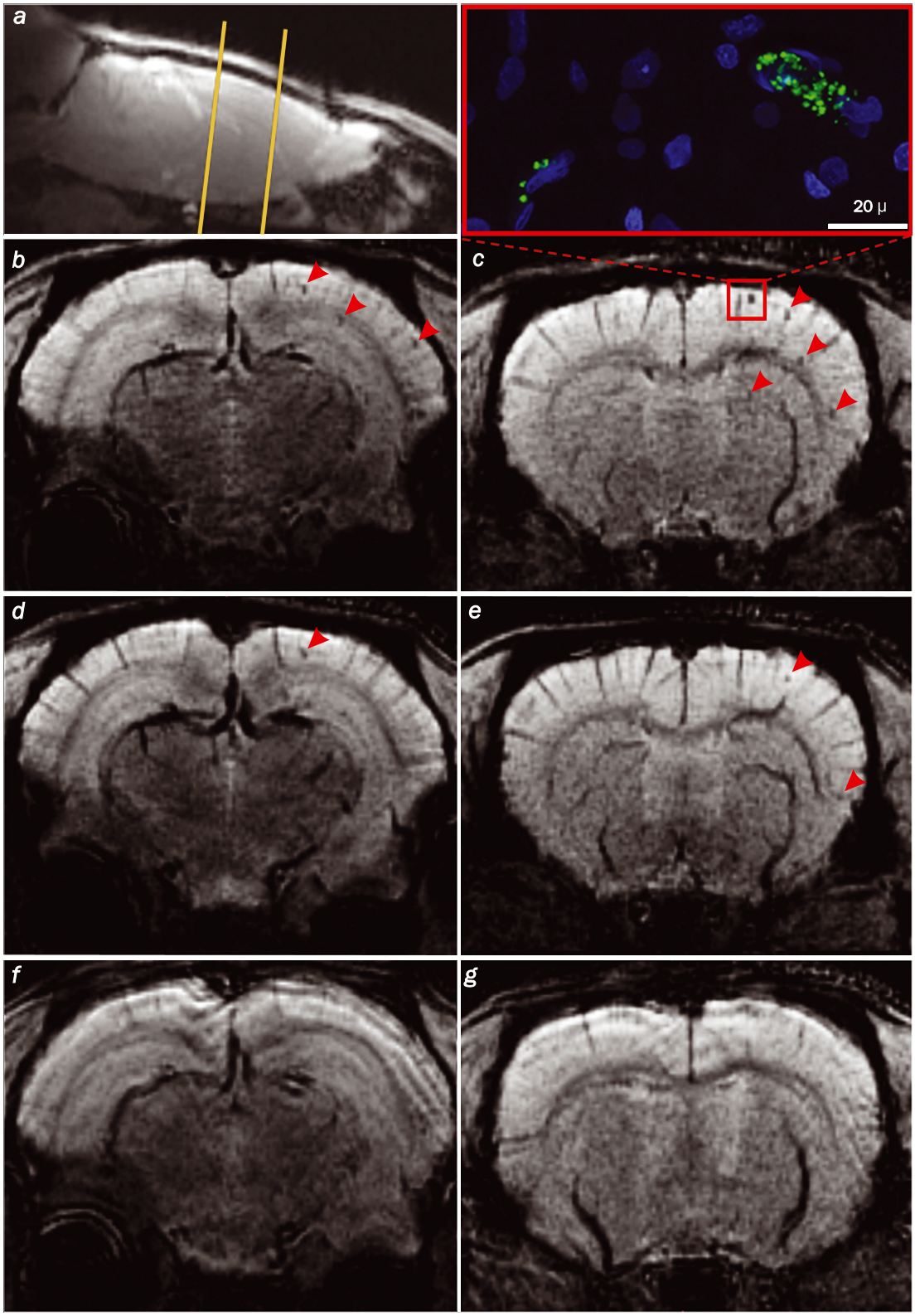

Fig. 3. MSC distribution in the brain of healthy rats after intra-arterial transplantation. Results of histological examination and MRI of the brain in dynamics from 1 to 72 h after transplantation. *a*) T2-weighted image in the sagittal projection, yellow lines show the position of axial MR images in SWI mode, shown on fragments *b*, *d*, *f* and *c*, *e*, *g*. *b*-*c*) Day 1 after MSC injection: Inset in fragment *b*: confocal microscopy; green fluorescence corresponds to SPIO-labeled cells. *d*-*e*) 48 h after MSC injection: *f*-*g*) 72 h after MSC injection: red arrows indicate hypointensive areas corresponding to labeled cells. The number of SPIO-labeled cells gradually decreases, and by 72 h, the cells were not detected.

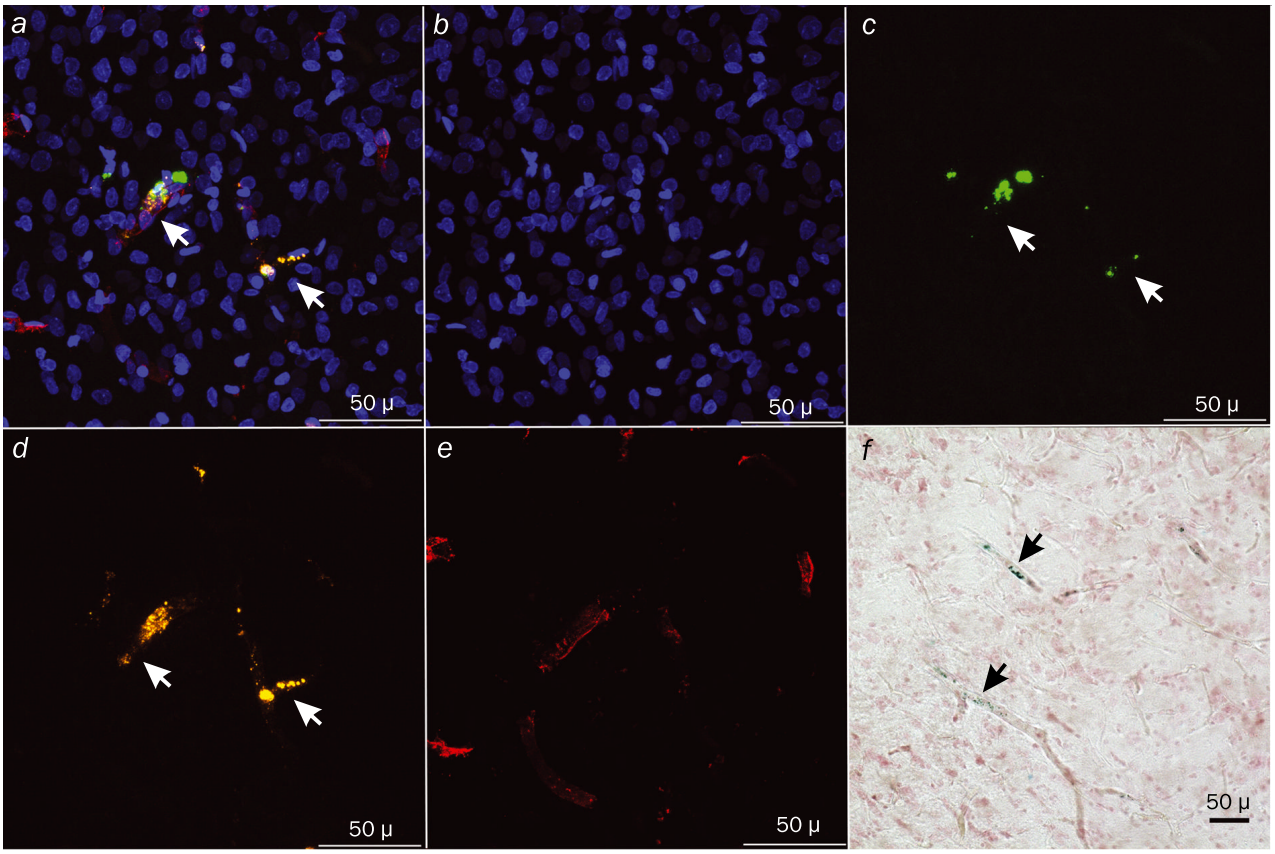

Fig. 4. Distribution and migration of MSC along blood vessels after intra-arterial injection to healthy rats. In 24 h after transplantation, MSC labeled with SPIO and lipophilic membrane dye PKH26 are visualized around cerebral vessels in contact with outer vascular walls. *a*) Combination of images *b*-*e*: DAPI+SPIO+PKH26+EBA (anti-Rat Blood-Brain Barrier Antibody); *b*) DAPI; *c*) SPIO; *d*) PKH26; *e*) EBA. *f*) Perls staining: arrows show transplanted cells in vessels.

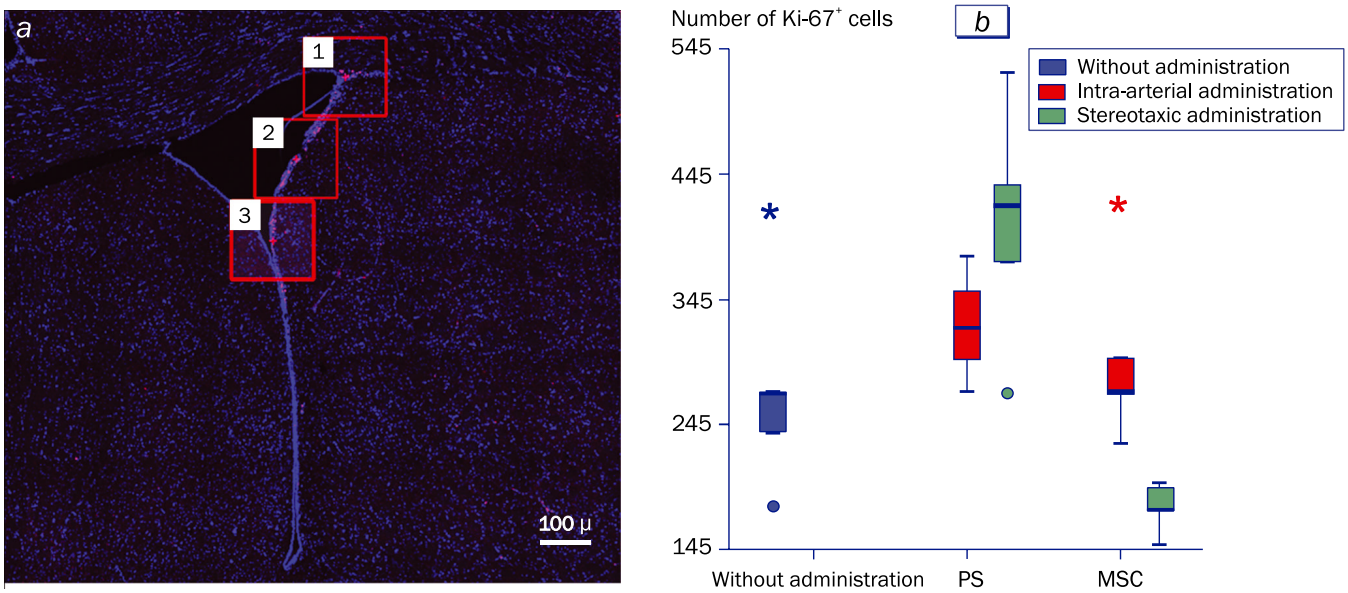

Fig. 5. Proliferative activity of endogenous cells in SVZ in healthy rats, depending on the administration route and substance administered. *a*) Brain section containing K-67$^+$cells: red frames: fields of cell counting. *b*) Dependence of Ki-67$^+$ cells number on the administration route and substance administered. Circles show outliers, *i.e.* values differing from the upper and lower quartiles by more than 1.5 interquartile intervals; asterisks show outliers differing by more than 2 interquartile intervals. Proliferation intensity after stereotaxic administration of PS was higher than in other groups.

of the cell cycle, except G0, and is used as the marker of proliferation [26]. According to our findings, only stereotaxic injection of PS increased cell proliferation in SVZ (the interaction of both factors is significant). After intra-arterial injection, neither PS, nor MSC significantly increased cell proliferation in SVZ. Interestingly, a tendency to a decrease in the number of proliferating cells relative to intact control was noted after intracerebral injection of MSC, but the differences were insignificant.

In our study, activation of cell proliferation on day 15 was revealed only after stereotaxic injection of PS, which can be regarded as a response to trauma caused by introduction of the needle and compression with additional volume. Activation of cell proliferation after neurotrauma was reported earlier [5]. However, our results did not confirm previous data [2,8] that MSC transplantation to laboratory animals stimulated cell proliferation in SVZ of the recipient brain, which is known to be a neurogenic zone [23]. This partial discrepancy between the results our findings and published data can be due to the fact that proliferation of endogenous cells in SVZ largely depends on the time and severity of brain injury. There is evidence that the intensity of neurogenesis greatly fluctuates during 2 months after injury and can sharply increase or decrease relative to the initial level [25]. To clarify this issue, studies of neurogenesis in dynamics, at different times after transplantation are requires. It can be assumed that the absence of differences and even a tendency to a decrease in proliferation intensity in intact animals and after stereotaxic administration of MSC can be associated with the therapeutic effect of MSC and the leveling of the effects of neurotrauma.

Thus, MSC from human placenta after stereotaxic administration to the brain of healthy rats can migrate long distance from the site of injection. Migration capacity of MSC and its rate depend on the tissue: in the corpus callosum, the cells pass considerable distances, whereas in the striatum and cortex, they practically remain at the injection site, although move and concentrate along the blood vessels. In case of intra-arterial transplantation into the internal carotid artery under conditions excluding capillary embolism, a small portion of transplanted MSC retained in the lumen of small arteries and capillaries of the brain (from few minutes to 2 days) and was also visualized in contact with the cerebral vessels, but from their inner side. The tropism of MSC to vessels can be explained by their similarity with pericytes [3]. The observed picture can reflect homing of MSC are homed into their own easily recognized niche [14].

The study was supported by the Russian Foundation for Basic Research (grant ofi_m 17-29-07045) and was performed on the equipment of Medical Nanobiotechnologies Common Use Center of the N. I. Pirogov Russian National Research Medical University, Common Use Centers of N. K. Koltsov Institute of Developmental Biology and V. N. Orekhovich Research Institute of Biomedical Chemistry.

REFERENCES

1. Abbott NJ, Patabendige AA, Dolman DE, Yusof SR, Begley DJ. Structure and function of the blood-brain barrier. Neurobiol. Dis. 2010;37(1):13-25.
2. Argibay B, Trekker J, Himmelreich U, Beiras A, Topete A, Taboada P, Pérez-Mato M, Vieites-Prado A, Iglesias-Rey R, Rivas J, Planas A.M, Sobrino T, Castillo J, Campos F. Intraarterial route increases the risk of cerebral lesions after mesenchymal cell administration in animal model of ischemia. Sci. Rep. 2017;7. ID 40758. doi: 10.1038/srep40758
3. Bouacida A, Rosset P, Trichet V, Guilloton F, Espagnolle N, Cordonier T, Heymann D, Layrolle P, Sensébé L, Deschaseaux F. Pericyte-like progenitors show high immaturity and engraftment potential as compared with mesenchymal stem cells. PLoS One. 2012;7(11). ID e48648. doi: 10.1371/journal.pone.0048648
4. Carman CV. Mechanisms for transcellular diapedesis: probing and pathfinding by invadosome-like protrusions. J. Cell Sci. 2009;122(Pt 17):3025-3035.
5. Chang EH, Adorjan I, Mundim MV, Sun B, Dizon ML, Szele FG. Traumatic brain injury activation of the adult subventricular zone neurogenic niche. Front. Neurosci. 2016;10. ID 332. doi: 10.3389/fnins.2016.00332
6. Coyne TM, Marcus AJ, Woodbury D, Black IB. Marrow stromal cells transplanted to the adult brain are rejected by an inflammatory response and transfer donor labels to host neurons and glia. Stem Cells. 2006;24(11):2483-2492.
7. Hasan A, Deeb G, Rahal R, Atwi K, Mondello S, Marei HE, Gali A, Sleiman E. Mesenchymal stem cells in the treatment of traumatic brain injury. Front. Neurol. 2017;8. ID 28. doi: 10.3389/fneur.2017.00028
8. Kan I, Barhum Y, Melamed E, Offen D. Mesenchymal stem cells stimulate endogenous neurogenesis in the subventricular zone of adult mice. Stem Cell Rev. Rep. 2011;7(2):404-412.
9. Khabbal J, Kerkelä E, Mitkari B, Raki M, Nystedt J, Mikkonen V, Bergström K, Laitinen S, Korhonen M, Jolkkonen J. Differential clearance of rat and human bone marrow-derived mesenchymal stem cells from the brain after intra-arterial infusion in rats. Cell Transplant. 2015;24(5):819-828.
10. Kholodenko IV, Konieva AA, Kholodenko RV, Yarygin KN. Molecular mechanisms of migration and homing of intravenously transplanted mesenchymal stem cells. J. Regen. Med. Tissue Eng. 2013;2(4). doi: 10.7243/2050-1218-2-4
11. Kim D, Chun BG, Kim YK, Lee YH, Park CS, Jeon I, Cheong C, Hwang TS, Chung H, Gwag BJ, Hong KS, Song J. In vivo tracking of human mesenchymal stem cells in experimental stroke. Cell Transplant. 2008;16(10):1007-1012.
12. Lam PK, Lo AW, Wang KK, Lau HC, Leung KK, Li KT, Lai PB, Poon WS. Transplantation of mesenchymal stem cells to the brain by topical application in an experimental traumatic brain injury model. J. Clin. Neurosci. 2013;20(2):306-309.

13. Laroni A, de Rosbo N.K, Uccelli A. Mesenchymal stem cells for the treatment of neurological diseases: Immunoregulation beyond neuroprotection. Immunol Lett. 2015;168(2):183-190.
14. Leibacher J, Henschler R. Biodistribution, migration and homing of systemically applied mesenchymal stem/stromal cells. Stem Cell Res. Ther2016;7. doi: 10.1186/s13287-015-0271-2
15. Li JM, Zhu H, Lu S, Liu Y, Li Q, Ravenscroft P, Xu YF, Huang L, Ma CM, Bezard E, Zhao RC, Wang RZ, Qin C. Migration and differentiation of human mesenchymal stem cells in the normal rat brain. Neurol. Res. 2011;33(1):84-92.
16. Liu L, Eckert MA, Riazifar H, Kang DK, Agalliu D, Zhao W. From blood to the brain: can systemically transplanted mesenchymal stem cells cross the blood-brain barrier? Stem Cells Int. 2013;2013. ID 435093. doi: 10.1155/2013/435093
17. Lo Furno D, Mannino G, Giuffrida R. Functional role of mesenchymal stem cells in the treatment of chronic neurodegenerative diseases. J. Cell. Physiol. 2018;233(5):3982-3999.
18. Matsushita T, Kibayashi T, Katayama T, Yamashita Y, Suzuki S, Kawamata J, Honmou O, Minami M, Shimohama S. Mesenchymal stem cells transmigrate across brain microvascular endothelial cell monolayers through transiently formed inter-endothelial gaps. Neurosci. Lett. 2011;502(1):41-45.
19. McGinley LM, Kashlan ON, Chen KS, Bruno ES, Hayes JM, Backus C, Feldman S, Kashlan BN, Johe K, Feldman EL. Human neural stem cell transplantation into the corpus callosum of Alzheimer's mice. Ann. Clin. Transl. Neurol. 2017;4(10):749-755.
20. Mitkari B, Kerkelä E, Nystedt J, Korhonen M, Mikkonen V, Huhtala T, Jolkkonen J. Intra-arterial infusion of human bone marrow-derived mesenchymal stem cells results in transient localization in the brain after cerebral ischemia in rats. Exp. Neurol. 2013;239:158-162.
21. Namestnikova D, Gubskiy I, Kholodenko I, Melnikov P, Sukhinich K, Gabashvili A, Vishnevskiy D, Soloveva A, Abakumov M, Vakhrushev I, Lupatov A, Chekhonin V, Gubsky L, Yarygin K. Methodological aspects of MRI of transplanted superparamagnetic iron oxide-labeled mesenchymal stem cells in live rat brain. PLoS One. 2017;12(10). ID e0186717. doi: 10.1371/journal.pone.0186717
22. Namestnikova D, Gubskiy I, Vishnevskiy D, Soloveva A, Vitushev E, Chekhonin V, Gubsky L, Gabashvili A, Yarygin K, Sukhinich K, Melnikov P. MRI evaluation of frequent complications after intra-arterial transplantation of mesenchymal stem cells in rats. J. Physics: Conf. Ser. 2017;886(1). ID 012012. doi: 10.1088/1742-6596/886/1/012012
23. Obernier K, Alvarez-Buylla A. Neural stem cells: origin, heterogeneity and regulation in the adult mammalian brain. Development. 2019;146(4). pii: dev156059. doi: 10.1242/dev.156059
24. Ryan JM, Barry FP, Murphy JM, Mahon BP. Mesenchymal stem cells avoid allogeneic rejection. J. Inflamm. (Lond). 2005;2. ID 8.
25. Saha B, Peron S, Murray K, Jaber M, Gaillard A. Cortical lesion stimulates adult subventricular zone neural progenitor cell proliferation and migration to the site of injury. Stem Cell Res. 2013;11(3):965-977.
26. Schlüter C, Duchrow M, Wohlenberg C, Becker MH, Key G, Flad HD, Gerdes J. The cell proliferation-associated antigen of antibody Ki-67: a very large, ubiquitous nuclear protein with numerous repeated elements, representing a new kind of cell cycle-maintaining proteins. J. Cell Biol. 1993;123(3):513-522.
27. Schmidt A, Ladage D, Steingen C, Brixius K, Schinköthe T, Klinz FJ, Schwinger RH, Mehlhorn U, Bloch W. Mesenchymal stem cells transmigrate over the endothelial barrier. Eur. J. Cell Biol. 2006;85(11):1179-1188.
28. Sukhinich KK, Kosykh AV, Aleksandrova MA. Differentiation and cell-cell interactions of neural progenitor cells transplanted into intact adult brain. Bull. Exp. Biol. Med. 2015;160(1):115-122.
29. Zheng H, Zhang B, Chhatbar PY, Dong Y, Alawieh A, Lowe F, Hu X, Feng W. Mesenchymal stem cell therapy in stroke: a systematic review of literature in pre-clinical and clinical research. Cell Transplant. 2018;27(12):1723-1730.